Comparison of 6-DOF Trajectory Model with Modified Linear Theory for Bullets

Dimitrios N. Gkritzapis,[a,b] Elias E. Panagiotopoulos,[c] Dionissios P. Margaris[c] and Dimitrios Papanikas[c]

[a] Captain of Hellenic Police, Laboratory of Firearms and Tool Marks Section, Criminal Investigation Division, Hellenic Police, 11522 Athens, Greece

[b] Hellenic Military Academy, and Mechanical Engineering and Aeronautics Dept., University of Patras, Greece

Email: gritzap@yahoo.gr

[c] Mechanical Engineering and Aeronautics Dept, University of Patras, 26500 Patras, Greece

Abstract: *A modified linear model is proposed for fast and accurate prediction of short and long-range trajectories of spin-stabilized bullets via atmospheric flight to a final impact point. This model is compared with a full 6-DOF trajectory model. The computational flight analysis takes into consideration the Mach number and total angle of attack effects by means of the variable aerodynamic coefficients.*

Keywords: *Low and high pitch angles, projectile trajectory, variable aerodynamic coefficients*

Introduction

External ballistics[1] deals with the behavior of a non-powered projectile in flight. Several forces act upon the projectile during this phase including gravity and air resistance.

Various authors have extended the projectile model for lateral force impulses,[2] as well as aerodynamic jump extending analysis due to lateral impulses[3] and aerodynamic asymmetry,[4] instability of controlled projectiles in ascending or descending flight.[5] Costello's modified linear theory[6] has also been applied recently for rapid trajectory projectile prediction.

The present work proposes several modifications to the full six degrees of freedom (6-DOF) theory that significantly improve the accuracy of impact point prediction of short and long range trajectories with variable aerodynamic coefficients of spin-stabilized bullets. For the purposes of the analysis, linear interpolation has been applied from the tabulated database of McCoy's text.[1]

Projectile model

The present analysis considers a 0.30 caliber (0.308 inch diameter), 168 grain (~10.9 g) Sierra International bullet used by National Match M14 rifle and loaded into 7.62 mm M852 match ammunition for high power rifle competition shooting, as shown in Figure 1. This bullet is not for combat use. The basic physical and geometrical characteristic data of the above mentioned 7.62 mm bullet are illustrated briefly in Table 1.

Trajectory flight simulation model

A six degrees of freedom rigid-projectile model[7–10] has been employed in order to predict the "free"

Figure 1. *7.62 mm match ammunition with a diameter of 0.30 caliber: representative small bullet types.*

Article Details	*Article No: - 0064*
Manuscript Received:-17/4/2008	*Final Revisions:-1/7/2008*
Publication Date:-18/7/2008	*Archive Reference:-574*

Table 1. *Physical and geometrical data of 7.62 mm bullet type.*

Characteristics	7.62 mm M852 bullet
Reference diameter/mm	7.62
Total length/mm	71.88
Total mass/kg	0.385
Axial moment of inertia/kg m^2	7.2282×10^{-8}
Transverse moment of inertia/kg m^2	5.3787×10^{-7}
Center of gravity from the base/mm	12.03

nominal atmospheric trajectory to final target area without any control practice runs. The six degrees of freedom in the flight analysis comprise the three translation components (x, y, z) describing the position of the projectile's center of mass and three Euler angles (φ, θ, ψ) describing the orientation of the projectile body as shown in Figure 2.Two main coordinate systems are used for the computational approach of the atmospheric flight motion. The one is a plane fixed (inertial frame, IF) at the firing site. The other is a no-roll rotating coordinate system on the projectile body (no-roll-frame, NRF, $\varphi = 0$) with the X_{NRF} axis along the projectile axis of symmetry and Y_{NRF}, Z_{NRF} axes oriented so as to complete a right hand orthogonal system. If the independent variable is changed from time t to dimensionless arc length l measured in calibers of travel:

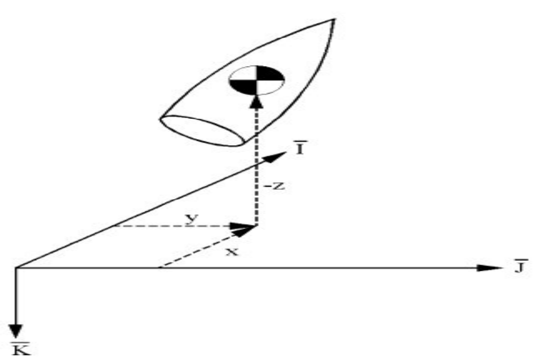

Figure 2. *No-roll (moving) and earth-fixed (inertial) coordinate systems for the projectile trajectory analysis.*

$$l = \frac{1}{D} s = \frac{1}{D} \int_0^t V_T \mathrm{d}t \qquad (1)$$

Equations (2)–(13) are the 6-DOF atmospheric equations of motion expressed in the no-roll frame.

The aerodynamic coefficients C_{D}, C_{La}, C_{MPA}, C_{MQ}, C_{MA} used in this model are projectile-specific functions of the Mach number and total angle of attack variations.

The projectile dynamics trajectory model consists of twelve non-linear first order ordinary differential equations, which are solved simultaneously by resorting to numerical integration using a 4th order Runge–Kutta method and with regard to the 6-D nominal atmospheric motion.

Modified trajectory model

Modified linear theory[10,15] makes several assumptions regarding the relative size of different quantities to further simplify the analysis: the Euler angle ψ is small so $\sin\psi \approx \psi$, $\cos\psi \approx 1$. The axial velocity $\tilde{u}_{\mathrm{NRF}}$ is replaced by the total velocity V_T because the side velocities $\tilde{v}_{\mathrm{NRF}}$ and $\tilde{w}_{\mathrm{NRF}}$ are small. The aerodynamic angles of attack α and sideslip β are small for the main part of the atmospheric trajectory.

The projectile is mass-balanced such that $I_{XY} = I_{YZ} = I_{XZ} = 0$, $I_{YY} = I_{ZZ}$. Quantities V_T and φ are large compared to ψ, $\tilde{q}_{\mathrm{NRF}}$, $\tilde{r}_{\mathrm{NRF}}$, $\tilde{v}_{\mathrm{NRF}}$ and $\tilde{w}_{\mathrm{NRF}}$, such that products of small quantities and their derivatives are negligible. In projectile linear theory, the Magnus forces in equations (9) and (10) are typically regarded as small and dropped. Magnus moments are due to the fact that a cross

$$x'_{\mathrm{IF}} = \frac{D}{V_T}\cos\psi\cos\theta\tilde{u}_{\mathrm{NRF}} - \frac{D}{V_T}\sin\psi\,\tilde{v}_{\mathrm{NRF}} + \frac{D}{V_T}\cos\psi\sin\theta\tilde{w}_{\mathrm{NRF}} \tag{2}$$

$$y'_{\mathrm{IF}} = \frac{D}{V_T}\cos\theta\sin\psi\tilde{u}_{\mathrm{NRF}} + \frac{D}{V_T}\cos\psi\tilde{v}_{\mathrm{NRF}} + \frac{D}{V_T}\sin\psi\sin\theta\tilde{w}_{\mathrm{NRF}} \tag{3}$$

$$z'_{\mathrm{IF}} = -\frac{D}{V_T}\sin\theta\tilde{u}_{\mathrm{NRF}} + \frac{D}{V_T}\cos\theta\tilde{w}_{\mathrm{NRF}} \tag{4}$$

$$\varphi' = \frac{D}{V_T}\tilde{p}_{\mathrm{NRF}} + \frac{D}{V_T}\tan\theta\,\tilde{r}_{\mathrm{NRF}} \tag{5}$$

$$\theta' = \frac{D}{V_T}\tilde{q}_{\mathrm{NRF}} \tag{6}$$

$$\psi' = \frac{D}{V_T\cos\theta}\tilde{r}_{\mathrm{NRF}} \tag{7}$$

$$\tilde{u}'_{NRF} = -\frac{D}{V_T}g\sin\theta - L_1 V_T C_D + \tilde{v}_{\mathrm{NRF}}\frac{D}{V_T}\tilde{r}_{\mathrm{NRF}} - \tilde{q}_{\mathrm{NRF}}\frac{D}{V_T}\tilde{w}_{\mathrm{NRF}} \tag{8}$$

$$\tilde{v}'_{NRF} = -L_1\left(C_{\mathrm{La}}+C_{\mathrm{D}}\right)\tilde{v}_{\mathrm{NRF}} - \frac{D}{V_T}\tilde{r}_{\mathrm{NRF}}\tilde{w}_{\mathrm{NRF}}\tan\theta - \frac{D}{V_T}\tilde{u}_{\mathrm{NRF}}\tilde{r}_{\mathrm{NRF}} \tag{9}$$

$$\tilde{w}'_{NRF} = \frac{D}{V_T}g\cos\theta - L_1\left(C_{\mathrm{La}}+C_{\mathrm{D}}\right)\tilde{w}_{\mathrm{NRF}} + \tilde{u}_{\mathrm{NRF}}\frac{D}{V_T}\tilde{q}_{\mathrm{NRF}} + \tan\theta\frac{D}{V_T}\tilde{r}_{\mathrm{NRF}}\tilde{v}_{\mathrm{NRF}} \tag{10}$$

$$\tilde{p}'_{\mathrm{NRF}} = D^5\frac{\pi}{16I_{XX}}\tilde{p}_{\mathrm{NRF}}\rho C_{\mathrm{LP}} \tag{11}$$

$$\begin{aligned}\tilde{q}'_{NRF} &= 2L_2\left(C_{\mathrm{La}}+C_{\mathrm{D}}\right)\tilde{w}_{\mathrm{NRF}}L_{\mathrm{CGCP}} + D\frac{L_2}{V_T}C_{\mathrm{MPA}}\tilde{p}_{\mathrm{NRF}}\tilde{v}_{\mathrm{NRF}}L_{\mathrm{CGCM}} + \\ &+ D^2L_2C_{\mathrm{MQ}}\tilde{q}_{\mathrm{NRF}} + 2D\,L_2C_{\mathrm{MA}} - \frac{D}{V_T}\tilde{r}_{\mathrm{NRF}}\frac{I_{XX}}{I_{YY}}\tilde{p}_{\mathrm{NRF}} - \frac{D}{V_T}\tilde{r}^2_{\mathrm{NRF}}\tan\theta\end{aligned} \tag{12}$$

$$\begin{aligned}\tilde{r}'_{\mathrm{NRF}} &= -2L_2\left(C_{\mathrm{La}}+C_{\mathrm{D}}\right)\tilde{v}_{\mathrm{NRF}}L_{\mathrm{CGCP}} + D\frac{L_2}{V_T}\tilde{p}_{\mathrm{NRF}}C_{\mathrm{MPA}}\tilde{w}_{\mathrm{NRF}}L_{\mathrm{CGCM}} + \\ &+ D^2L_2C_{\mathrm{MQ}}\tilde{r}_{\mathrm{NRF}} - 2DL_2C_{\mathrm{MA}} + \frac{D}{V_T}\tilde{p}_{\mathrm{NRF}}\tilde{q}_{\mathrm{NRF}}\frac{I_{XX}}{I_{YY}} + \frac{D}{V_T}\tilde{q}_{\mathrm{NRF}}\tilde{r}_{\mathrm{NRF}}\tan\theta\end{aligned} \tag{13}$$

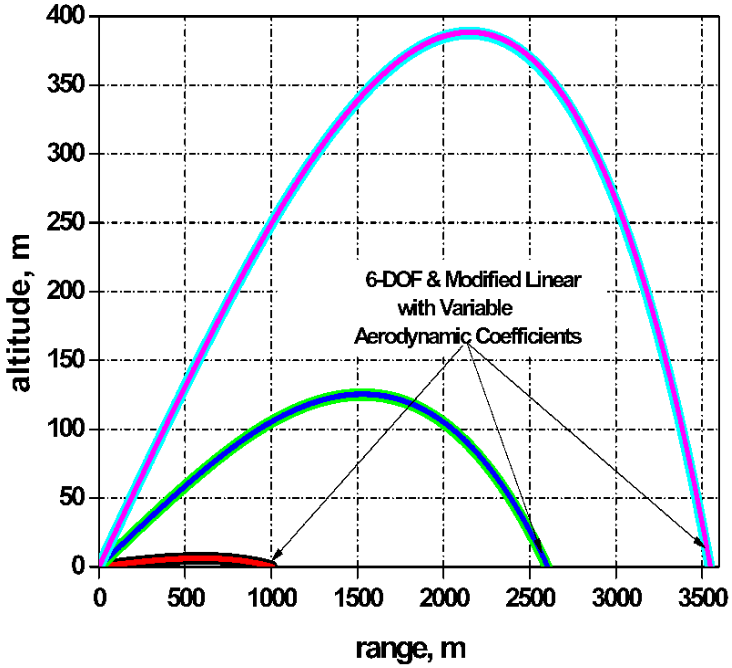

Figure 3. *Flight paths of 7.62 mm bullet at pitch angles of 1, 7 and 15 degrees for 6-DOF and modified linear models.*

product between the Magnus force and its respective moment arm is not necessarily small. With the aforementioned assumptions, the above expressions results in equations (2i)–(13i):

The equations 5, 6, 7 and 11 remain invariable.

The modified linear trajectory model runs at faster time with variable aerodynamic coefficients than the corresponding full 6-DOF analysis. On the other hand 6-DOF gives results of high accuracy trajectory prediction.

$$x'_{\mathrm{IF}} = D\cos\theta \tag{2i}$$

$$y'_{\mathrm{IF}} = D\cos\theta\psi \tag{3i}$$

$$z'_{\mathrm{IF}} = -D\sin\theta \tag{4i}$$

$$V'_T = -\frac{D}{V_T} g\sin\theta - L_1 V_T C_D \tag{8i}$$

$$\tilde{v}'_{\mathrm{NRF}} = -L_1\left(C_D + C_{\mathrm{La}}\right)\left(\tilde{v}_{\mathrm{NRF}} - \tilde{v}_w\right) - D\tilde{r}_{\mathrm{NRF}} \tag{9i}$$

$$\tilde{w}'_{\mathrm{NRF}} = \frac{D}{V_T} g\cos\theta - L_1\left(C_{\mathrm{D}} + C_{\mathrm{La}}\right)\left(\tilde{w}_{\mathrm{NRF}} - \tilde{w}_w\right) + D\tilde{q}_{\mathrm{NRF}} \tag{10i}$$

$$\tilde{q}'_{\mathrm{NRF}} = 2L_2\left(C_{\mathrm{D}}+C_{\mathrm{La}}\right)\left(\tilde{w}_{\mathrm{NRF}}-\tilde{w}_w\right)L_{\mathrm{CGCP}} + + D\frac{L_2}{V_T}C_{\mathrm{MPA}}\,\tilde{p}_{\mathrm{NRF}}\left(\tilde{v}_{\mathrm{NRF}}-\tilde{v}_w\right)L_{\mathrm{CGCM}} + + D^2L_2C_{\mathrm{MQ}}\,\tilde{q}_{\mathrm{NRF}} + 2DL_2C_{\mathrm{MA}} \tag{12i}$$

$$\tilde{r}'_{\mathrm{NRF}} = -2L_2\left(C_{\mathrm{D}}+C_{\mathrm{La}}\right)\left(\tilde{v}_{\mathrm{NRF}}-\tilde{v}_w\right)L_{\mathrm{CGCP}} + + D\frac{L_2}{V_T}\tilde{p}_{\mathrm{NRF}}\,C_{\mathrm{MPA}}\left(\tilde{w}_{\mathrm{NRF}}-\tilde{w}_w\right)L_{\mathrm{CGCM}} + + D^2L_2C_{\mathrm{MQ}}\,\tilde{r}_{\mathrm{NRF}} - 2DL_2C_{\mathrm{MA}} \tag{13i}$$

Atmospheric model

Atmospheric properties of air, like density ρ, are being calculated based on a standard atmosphere from the International Civil Aviation Organization (ICAO).

Computational simulation

The flight dynamic model of a 7.62 mm bullet involves the solution of the set of twelve first order ordinary differentials for two trajectories with variable aerodynamic coefficients, first the full 6-DOF and second with simplifications for the modified trajectory, Equations (2)–(13), which are solved simultaneously by resorting to numerical integration using a 4th order Runge–Kutta method. The six-degrees-of-freedom and the modified linear model numerical trajectories were computed by using a time step size of 10×10^{-3} s. Initial flight conditions for both dynamic flight simulation models are illustrated in Table 2 for the test cases examined.

Results and Discussion

The flight path of 6-DOF trajectory motion[1] with variable[11] and no constant[12] aerodynamic coefficients of the 7.62 mm projectile with initial firing velocity of 792.48 m s^{-1}, rifling twist rate 1 turn in 12 inches (30 cm), at 1°, 7° and 15°, are indicated in Figure 3. The calculated impact points of the above no-wind trajectories with the proposed variable aerodynamic coefficients are compared with accurate estimations of modified linear trajectory analysis and provide quite good prediction of the entirety of the atmospheric flight motion for the same initial flight conditions.

Figure 4 shows the crossrange flight path of a 7.62 mm bullet downrange distance for both methods with no big differences in low launch angle but differences in high angles. At 1, 7 and 15 degrees pitch angle for 6-DOF we have values of the crossrange as 3.94 cm, 7.2 m and 24.3 m, respectively. For the same initial conditions the modified theory has the values 3.9 cm, 6.9 m, and 22 m, respectively.

Figure 5 shows that the velocity *versus* range diagrams of the two methods, at initial pitch angles of 1, 7 and 15 degrees, have no differences. Figure 6 also shows that the trajectory analysis for the three roll rates is the same for the 7.62 mm

Table 2. *Initial flight parameters of the bullet test case examined.*

Initial flight data	7.62 mm M852 bullet
x/m	0.0
y/m	0.0
z/m	0.0
φ/deg	0.0
θ/deg	1, 7 and 15
ψ/deg	0.0
u/m s^{-1}	792.48
v/m s^{-1}	0.0
w/m s^{-1}	0.0
p/rad s^{-1}	16343.0
q/rad s^{-1}	0.0
r/rad s^{-1}	0.0

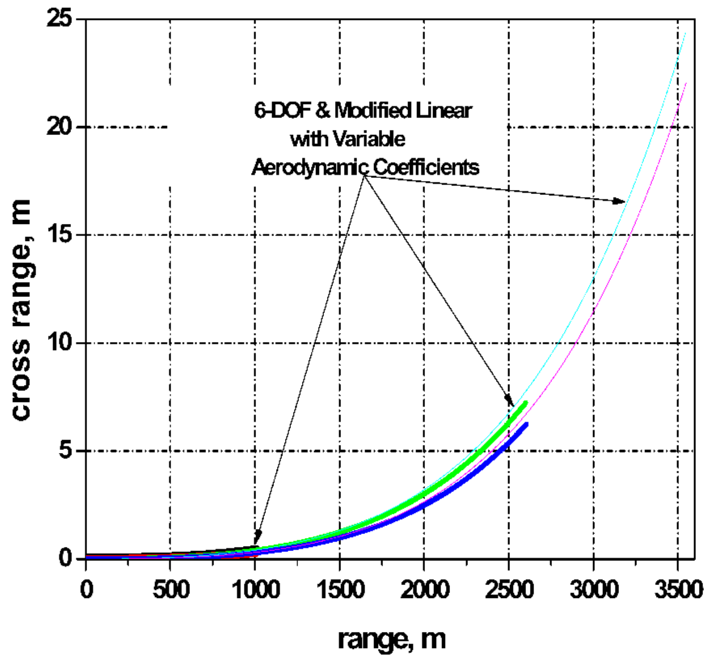

Figure 4. *Crossrange versus downrange distance of 7.62 mm bullet for modified linear and 6-DOF models*

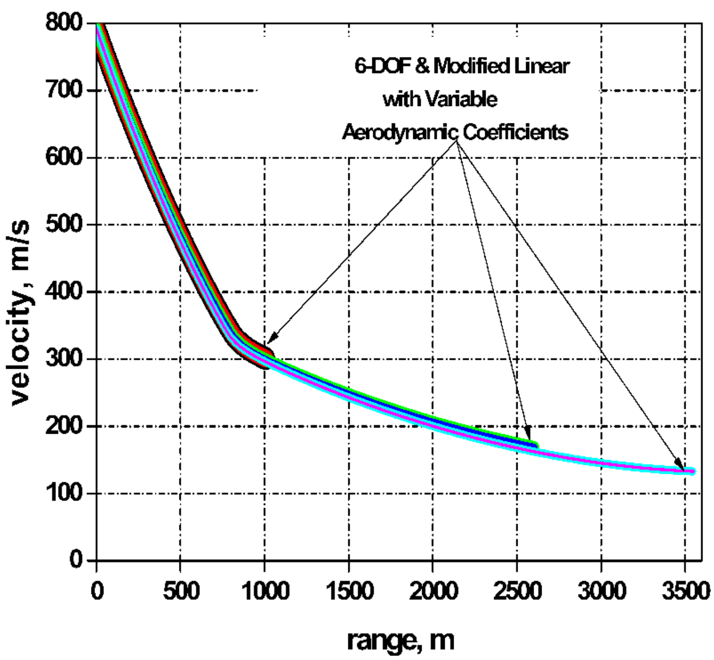

Figure 5. *Velocity versus range of 7.62 mm bullet for low and high pitch angles in the two trajectory models.*

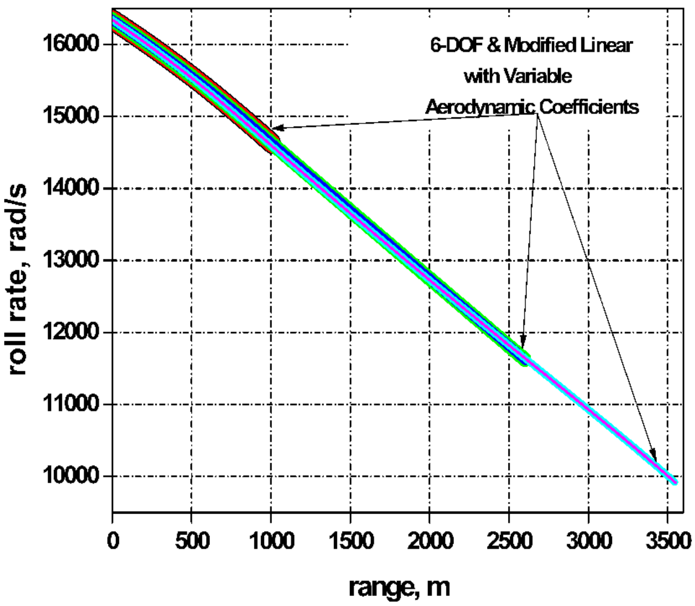

Figure 6. *Roll rates versus range of 7.62 mm bullet for modified linear and 6-DOF models.*

bullet with variable aerodynamic coefficients.

Conclusion

The modified linear trajectory model was shown to provide reasonable impact predictions at short and long-range trajectories of high and low spin-stabilized bullets. Moreover, the modified model showed some differences at high pitch angles. However, the comparison between the 6-DOF and the modified trajectory model provided quite good results with the variable aerodynamic coefficients over the whole flight path. The computational results of the proposed synthesized analysis are in good agreement compared with other technical data and recognized exterior atmospheric projectile flight computational models.

References

1 R. McCoy, *Modern Exterior Ballistics*, Schiffer, Attlen, PA, 1999.

2 B. Burchett, A. Peterson and M. Costello, "Prediction of Swerving Motion of a Dual-Spin Projectile with Lateral Pulse Jets in Atmospheric Flight," *Mathematical and Computer Modeling*, Vol. 35, No. 1–2, 2002.

3 G. Cooper, *Projectile Aerodynamic Jump Due to Lateral Impulsives*, Army Research Laboratory, ARL-TR-3087, 2003.

4 G. Cooper, *Extending the Jump Analysis for Aerodynamic Asymmetry*, Army Research Laboratory, ARL-TR-3265, 2004.

5 C. Murphy, "Instability of Controlled Projectiles in Ascending or Descending Flight," *Journal of Guidance, Control, and Dynamics*, Vol. 4, No. 1, 1981.

6 L. Hainz and M. Costello, "Modified Projectile Linear Theory for Rapid Trajectory Prediction," *Journal of Guidance, Control, and Dynamics*, Vol. 28, No. 5, 2005.

7 B. Etkin, *Dynamics of Atmospheric Flight*, John Wiley and Sons, New York, 1972.

8 K. Joseph, M. Costello and S. Jubaraj, *Generating an Aerodynamic Model for Projectile Flight Simulation Using Unsteady Time Accurate Computational Fluid Dynamic Results*, Army Research Laboratory, ARL-CR-577, 2006.

9 M. J. Amoruso, "Euler Angles and Quaternions in Six Degree of Freedom Simulations of Projectiles," Technical Note, 1996.

10 M. Costello and D. Anderson, "Effect of

Internal Mass Unbalance on the Terminal Accuracy and Stability of a projectile," *AIAA Paper*, 1996.

11 D. N. Gkritzapis, E. E. Panagiotopoulos, D. P. Margaris and D. G. Papanikas, "Atmospheric Flight Dynamic Simulation Modeling Of Spin-Stabilized Projectiles," *Journal of Pyrotechnics*, Issue 26, Winter 2007, pp. 3–14.

12 D. N. Gkritzapis, E. E. Panagiotopoulos, D. P. Margaris and D. G. Papanikas, "Atmospheric Flight Dynamic Simulation Modeling Of Spin-Stabilized Projectiles and Small Bullets with Constant Aerodynamic Coefficients," *Journal of Pyrotechnics*, Issue 26, Winter 2007, pp. 15–22.

Nomenclature

C_{D}	drag force aerodynamic coefficient
C_{LP}	lift force aerodynamic coefficient
C_{La}	roll damping moment aerodynamic coefficient
C_{MQ}	pitch damping moment aerodynamic coefficient
C_{MA}	overturning moment aerodynamic coefficient
C_{MPA}	Magnus moment aerodynamic coefficient
$x'_{\mathrm{if}}, y'_{\mathrm{if}}, z'_{\mathrm{if}}$	projectile position coordinates in the inertial frame/m
m	projectile mass/kg
D	projectile reference diameter/m
s	dimensionless arc length
V_{T}	total aerodynamic velocity/m s^{-1}
$\tilde{u}_{\mathrm{NRF}}, \tilde{v}_{\mathrm{NRF}}, \tilde{w}_{\mathrm{NRF}}$	projectile velocity components expressed in the no-roll-frame/m s^{-1}
$\tilde{u}_{\mathrm{w}}, \tilde{v}_{\mathrm{w}}, \tilde{w}_{\mathrm{w}}$	wind velocity components in no-roll-body-frame/m s^{-1}
$\tilde{p}_{\mathrm{NRF}}, \tilde{q}_{\mathrm{NRF}}, \tilde{r}_{\mathrm{NRF}}$	projectile roll, pitch and yaw rates in the moving frame, respectively/rad s^{-1}
ρ	density of air/kg m^{-3}
φ , θ, ψ	projectile roll, pitch and yaw angles, respectively/deg
α, β	aerodynamic angles of attack and sideslip
g	gravity acceleration/m s^{-2}
I	projectile inertia matrix
I_{XX}	projectile axial moment of inertia/kg m^{-2}
I_{YY}	projectile transverse moment of inertia about y-axis through the center of mass/kg m^2
I_{XX}, I_{YY}, I_{ZZ}	diagonal components of the inertia matrix
I_{XY}, I_{YZ}, I_{XZ}	off-diagonal components of the inertia matrix
L_{CGCM}	distance from the center of mass (CG) to the Magnus center of pressure (CM) along the station line/m
L_{CGCP}	distance from the center of mass (CG) to the aerodynamic center of pressure (CP) along the station line/m
L_1, L_2	dimensional coefficients, $\pi\rho D^3/8m$ and $\pi\rho D^3/16I_{YY}$, respectively